Building a Bacterial Biosensor for the Detection of Synthetic Opioids

A Major Qualifying Project Report
Submitted to the Faculty of
WORCESTER POLYTECHNIC INSTITUTE
In partial fulfillment of the requirements for the
Degree of Bachelor of Science
In Biology and Biotechnology

By: Amanda Maffeo

Approved: Natalie G. Farny, PhD
Biology and Biotechnology
Project Advisor

Abstract

Fentanyl is a synthetic opioid, 50 to 100 times more potent than heroin and morphine, which contributes to the thousands of overdoses that occur each year in the United States. With a drug as dangerous as fentanyl, it is important to be able to detect it quickly and accurately. Many biosensors used for the detection of narcotics today are expensive and limited. In order to detect fentanyl in a rapid and cost-effective way, a genetic circuit in *E. coli* was designed with the capability of sensing fentanyl in water samples. The efficiency and sustainability of circuit induction under low nutrient conditions was tested. The fentanyl biosensor has the ability for traces of drugs to be detected within a community's water allowing the use of narcotics in that area to be monitored.

Acknowledgements

I would like to acknowledge the following people who made this project possible.

- Professor Natalie Farny for her guidance and support over the course of this project.
- WPI for providing laboratory space and financial support.

Table of Contents

Introduction

Pharmaceutical Pollution

The growing opioid epidemic is a public health crisis, which takes about 130 lives each day. There are many facets to the opioid epidemic, including drug use, over-prescription, and distribution, but also impacts to the environment (USA Facts, 2019). Measurable amounts of prescription drugs have been found in 80% of water sources in 30 states (Drugs in the Water, 2011). With the growing use of prescription medications, these amounts can be expected to grow. An experiment conducted in Seattle used muscles to detect the drug pollution in the waters. Over time, the muscles tested positive for opioids, raising concern for alternative modes of opioid ingestion (Miller, 2018). While this growing contamination has not yet reached harmful concentration levels, the movement of opioids through wastewater poses threats to humans and other organisms in contact with the water.

The presence of opioids in wastewater also brings about opportunity. Detectable traces of drugs within a community's water allows the use of narcotics in that area to be monitored. The use of wastewater epidemiology allows for collected data to create a forecast for expected opioid related overdose and death (Gushgari et al., 2019). This information is pertinent in understanding opioid use in the US, as it is directly correlated to opioid analyte concentrations observed in wastewater via wastewater epidemiology.

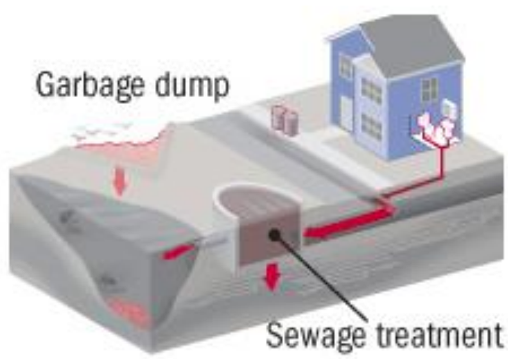

Figure 1: Traces of prescription drugs make their way into water sources via wastewater. Fractions of the drugs that are not metabolized by the body are excreted through urine and feces. Drugs are also introduced when flushed down the toilet (Drugs in the Water, 2011).

Fentanyl

Fentanyl is a synthetic opioid, 50 to 100 times more potent than heroin and morphine, which contributes to the thousands of overdoses that occur each year in the United States. The increased use of opioids often begins as valid medical prescriptions to treat pain; however, studies have found that people unintentionally misuse opioids due to their highly addictive nature (NIH, 2020). In 2017, 59% of opioid related deaths involved fentanyl (NIH, 2019). Due to the extreme potency of the drug, a lethal dose is only 3 milligrams, compared to that of heroin at 30 milligrams (Truth about fentanyl). At such a low dosage, just coming into contact with fentanyl can be dangerous. These adverse effects include respiratory depression, asthma, and gastrointestinal obstruction (fentanyl(Rx), 2019). Fentanyl is often laced into other drugs such as heroin and cocaine without users' knowledge, creating more dangerous mixtures and increasing likelihood of overdose. Manufacturers have also started making chemical alterations to fentanyl, creating a more potent drug. An example of this is carfentanyl, which is 100 times more potent than fentanyl (Synthetic Opioid Overdose Data, 2019). This constant creation of similar drugs creates an uncertainty of what the drug actually is, how potent it is, and how it can effectively be detected.

With a drug as dangerous as fentanyl, it is important to be able to detect it quickly and accurately. Today, most modes of detection include chromatography, spectrophotometry, and various biosensors. Many of the methods used are time consuming and have questionable reliability and validity (Angelini et al., 2019). As mentioned above, many forms of fentanyl are manufactured, creating multiple isomers. Detection methods need to be able to adjust in order to have a generic recognition of fentanyl and fentanyl related drugs. It is important to create methods that are more than just a qualitative detection that simply reveal if there is the presence of a specific substance, and increase sensitivity to obtain quantitative results.

Biosensors

Biosensors are organisms or biological molecules used to detect the presence, and or the concentration of specific substances. These tools are genetically engineered to recognize specific targets, and produce a visual indication of its presence, often by generating a fluorescent protein. There is a wide array of biosensors, all having different uses and mechanisms. Due to their rapid, easy, and low-cost nature, they are useful in the advancement of point-of-care detection, as well as environmental monitoring (Kawamura and Miyata, 2016). Many biosensors used for the detection of narcotics today rely on molecular binding and antibody detection (Klenkar and Liedberg, 2008). While these methods do work, they often come in the form of a chip, or microelectronic, which need to be loaded with an aqueous sample (Gandhi et al., 2015). This form of testing is limited as it requires expensive laboratory equipment and reagents, as well as trained personnel. Ideally, in order to use biosensors more broadly to test for contaminated drug products and monitor wastewaters, the biosensors should be cost effective, easy to perform, and capable of being used in a field setting.

Using Synthetic Biology to Enhance Detection

The goal of this project is to develop a bacterial biosensor for the detection of fentanyl. Through the use of synthetic biology techniques, the genetic circuit designed will allow for a rapid and quantitative detection of this opioid. This advancement will provide the basis for a novel drug screening product that is rapid and cost-effective, eliminating the need to send away collected samples to laboratories and await results. This biosensor could be used in cases of emergency screenings associated with drug overdose, roadside testing, and environmental sampling, as well as wastewater epidemiology. Unlike current opioid detection methods that often reveal whether a substance is present in a sample or not, this sensor could provide insight into how much is present based on the amount of fluorescent protein produced. With the knowledge of the fentanyl structure and studied mechanisms used to modulate DNA circuits, this project is aiming to create an accurate and efficient means of detecting fentanyl.

Sustainability of Biosensors

An important aspect to consider in building a cell-based biosensor is the survival of bacterial cells in different sensing environments. Our goal in understanding the sustainability of bacterial biosensors is to see if the circuit is capable of induction after being grown in non-nutrient rich environments. Table 1 shows the results of a study that focused on the survival of multiple bacterial strains after storage in water and PBS. The results reveal that after many weeks of storage, the bacteria are capable of surviving in a media other than a nutrient rich LB. For the design of a bacterial biosensor with intentions of water testing, it is important to understand how the bacteria will respond to its environment. Knowing that the bacteria can survive in water allows us to realize the capabilities and the limitations of an inducible sensor.

	Log_{10} CFU ml^{-1} reduction (% survival)		
Bacteria	In water	In PBS	Difference*
Pseudomonas aeruginosa PAO1	2·67 (0·21)	2·27 (0·54)	0·40
Salmonella Mbandaka S14	2·56 (0·28)	2·82 (0·15)	−0·26
Listeria monocytogenes Scott A†	6·18 (< 0·01)	1·63 (2·34)	4·55
Pseudomonas fluorescens CY091 (Biovar II)	0·91 (12·35)	0·99 (10·24)	−0·08
Pseudomonas fluorescens LU-04-1B (Biovar IV)	1·82 (1·51)	1·94 (1·15)	0·12
Pseudomonas fluorescens BC-05-1B (Biovar V)	1·98 (1·04)	1·43 (3·71)	0·55
Pseudomonas putida ATCC 12633	2·22 (0·60)	1·92 (1·21)	0·30
Erwinia carotovora ssp. *carotovora* SR319	2·97 (0·11)	2·60 (0·25)	0·37
Xanthomonas campestris pv·*campestris* XC11	2·42 (0·38)	2·28 (0·52)	0·14

Table 1: The results above show the survival of multiple bacterial strains after 30 weeks of storage in water and PBS. Results show that bacteria are capable of surviving in non-nutrient rich environments for extended periods of time (Liao and Shollenberger, 2003).

Project Goal

Within this project there are two goals. The first, to construct a genetic circuit in *E. coli* capable of sensing fentanyl in water samples. The second, to measure the efficiency of genetic circuit induction under low nutrient conditions. Through background research an optimal design for the plasmid construct was pieced together in Benchling. Cloning and transformations were used in pursuit of assembling the complete circuit into *E. coli* cells. In order to understand induction capabilities in non-nutritive environments, *E. coli* cells expressing an existing arabinose biosensor were grown in non-nutritive conditions and induced and measured at various time points.

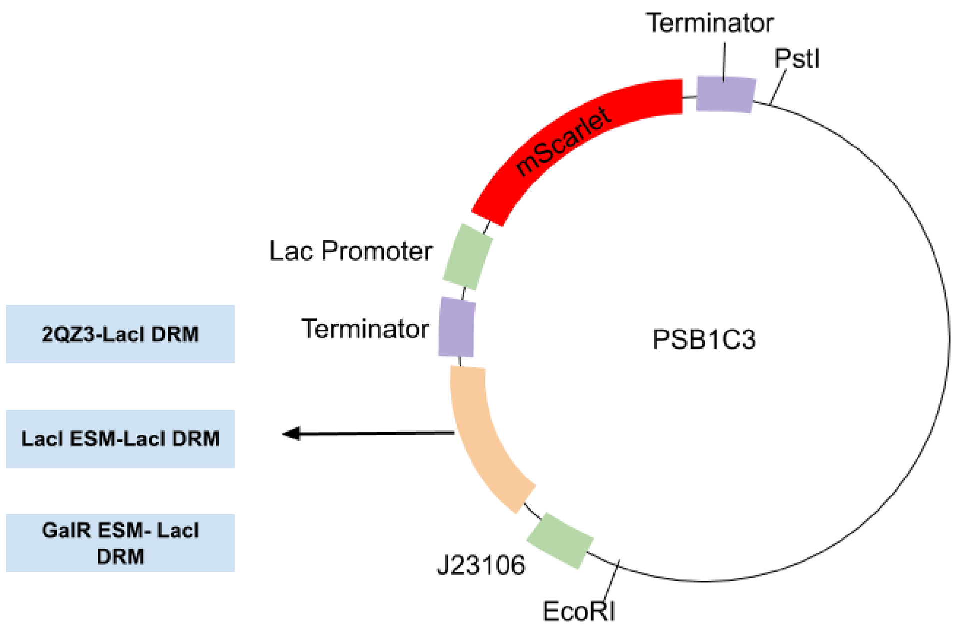

Figure 2: Schematic of genetic circuit.

The design of the sensor came from knowledge developed from a "Passcode circuit" (Chan et al., 2015). The passcode circuit functions to modularize DNA and create a versatile biocontainment system that is capable of detecting diverse signals. The practical use of this circuit allows for different combinations of input signals to control expression of the target gene. Through the rearrangement of the environmental sensing module (ESM) and DNA recognition module (DRM) of the transcription factors, the circuit can easily be reprogrammed to reconfigure sensing capabilities and transcriptional regulation. For the development of this project, the LacI-LacI circuit, as well as the LacI-GalR circuit were used. The use of the LacI and GalR ESM and DRM allowed the placement of a target gene into the vector, in order to transform the circuit into a fentanyl recognizing system.

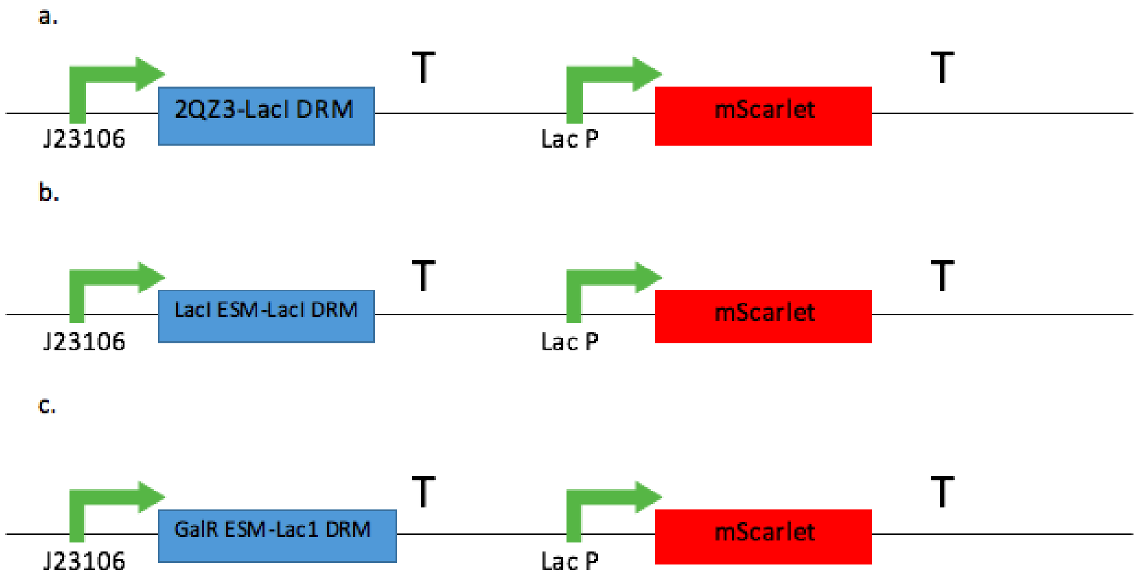

Figure 3: The graphic above shows the three target sequences to be inserted into the pSB1C3 backbone.

Another study reviewed introduced molecules similar to fentanyl, as well as ligand-binding proteins that are capable of detecting fentanyl. The paper focuses on 2QZ3, a protein scaffold that was found to bind xylotetraose, a sugar molecule similar in conformation to fentanyl (Bick et al., 2017). From this original parent scaffold, two conformers, Fen49 and Fen21, were created as mutations to 2QZ3. This protein complex with a high affinity for fentanyl was then engineered into plant cells in order to create an environmental sensor. These fentanyl binding proteins were then incorporated into a transcription factor based system, allowing them to activate transcription of a fluorescent reporter protein in response to fentanyl.

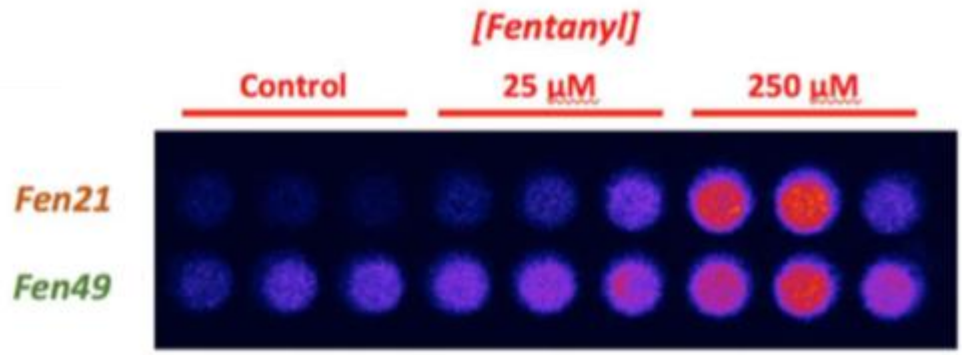

Figure 4: The figure above shows Fen 21 and Fen 49 when induced with fentanyl. As the concentration of fentanyl increases, a stronger expression of the fluorescent protein can be seen as the bright red glow. These results show not only a receptiveness to fentanyl but also a sensitivity that can provide a quantitative analysis (Bick et al., 2017).

By piecing this knowledge together, the design for this project was created. By understanding the pathways of the passcode circuit, the 2QZ3 sequence was placed into a vector with a pSB1C3 backbone and mScarlet fluorescence. With this circuit, molecules structurally similar to fentanyl will be able to be detected. We can then substitute the surrogate for fentanyl and gain the same results. Through these synthetic biology techniques and understandings, a biosensor capable of detecting fentanyl was designed and produced.

Methods

Plasmid Construction and Characterization

All plasmids were constructed using conventional protocols and Gibson Assembly. Genetic elements from the Passcode circuit (Chan et al., 2015), including the LacI and GalR ESM and DRM (Appendix A, Seq. 1, 2, 3) were used, alongside the 2QZ3 (Appendix A, Seq. 4) protein and mScarlet fluorescent protein (Appendix A, Seq. 5). Using EcoR and PstI, the target sequence was assembled into a pSB1C3 backbone. The constructed plasmids were transformed into competent DH5-alpha cells and plated on chloramphenicol plates (33 µg/mL). Minipreps were prepared from overnight cultures of selected colonies using Qiagen reagents. Miniprep samples were then analyzed via gel electrophoresis and sequence analysis.

Parallel to the 2QZ3 circuit, IPTG colonies were screened for the presence of mScarlet. Selected colonies were numbered and plated to both IPTG positive and negative plates with a final concentration of 1mM IPTG. Colonies were left to grow and analyzed visually for red coloration. Selected colonies were then miniprepped and analyzed via gel electrophoresis and sequence analysis.

Circuit Induction

Colonies for pSB1C3-I20270 (positive control), pSB1C3-Double Terminator (negative control), and pSB1C3-AraC-GFP were selected and grown overnight in 5mL LB with 5µL of 33 mg/mL chloramphenicol. A 1:10 dilution was made for each culture and the OD was measured. Two 10mL cultures were made for each circuit in LB, PBS, and water. Half of the samples were induced with 100µL of 0.1% arabinose and vortexed. At time points 0, 4, 24, and 72 (hours), 100µL of each culture was loaded into a 96 well plate (Appendix B). For LB cultures, 500µL were transferred to a microcentrifuge tube and centrifuged at 14,000 RPM for 5 mins. The supernatant was discarded and the bacteria was resuspended in 500µL of PBS. 100µL samples were loaded into the wells. Identical experiments were set with induction happening after 3 and 7 days.

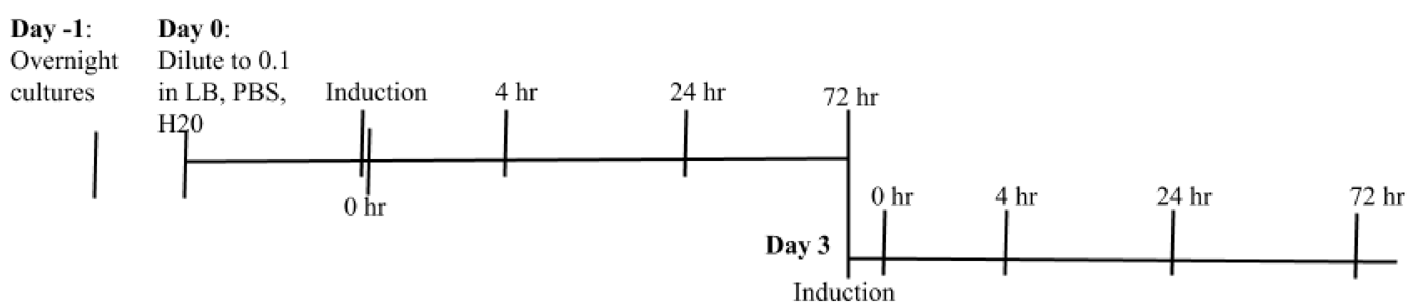

Figure 5: Above is a timeline showing the pattern for circuit induction. The same pattern was used for the 7 day induction samples, with induction happening on day 7.

Results

Fentanyl Biosensor Cloning

For this part of the experiment, cloning of the LacI-LacI circuit was attempted. Transformations were conducted several times, yielding no results. The circuits were redesigned with the goal of simplifying and decreasing the size of the plasmid insert. With continued trials, colonies began to grow; however, background expression was high on the negative control plate. It was expected that if the clones were functional, this would result in red colonies on the IPTG+ plate and not on the IPTG- plate. Screening for positive colonies was then done by plating some of the clones on IPTG positive and negative plates. These plates were then checked for the colonies that produced a stronger red color on the IPTG positive plate. Some colonies produced a red color even on the IPTG negative plates which showed that the LacI-LacI circuit had leaky transcription. Minipreps and test digests were done for these samples in order to examine the inserts. The test digests were tested via gel electrophoresis; however, results were inconclusive (Figure 6). Prepared minipreps did not have a high enough DNA concentration for sequencing.

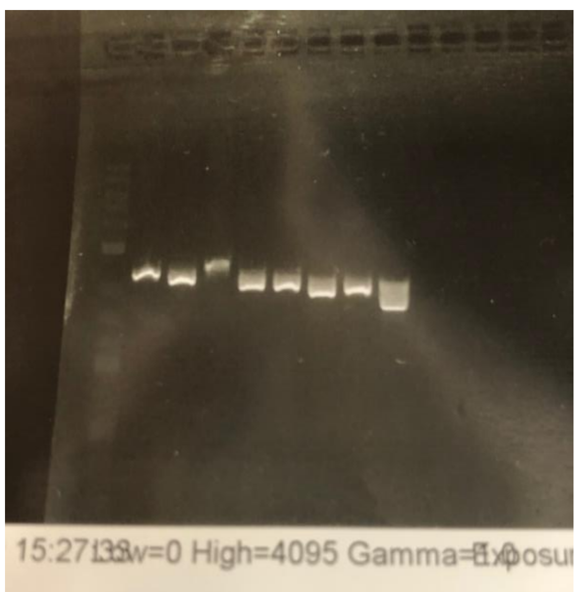

Figure 6: Picture of gel electrophoresis of test digest samples made from IPTG +/- plates. Two bands were expected to show, one for the vector and the other for the insert. Lane 9 is the only sample that could possess both bands and could be investigated further.

Fluorescence of AraC-GFP Circuit

With this part of the experiment, the goal was to measure induction and understand the capabilities of bacterial biosensors when grown in a limited nutrient environment, either PBS or water, versus LB. We used the pBAD-AraC arabinose inducible system for these experiments (Figure 7).

Figure 7: The arabinose circuit designed by a previous MQP team. The insert consisted of the constitutive promoter pRpoS, which drives the repressor AraC, which regulates GFP. This insert was placed in a pSB1C3 backbone. When induced with arabinose, GFP is expressed. (Martin et al., 2018)

Figure 7 shows that when the cultures were induced immediately after dilution from overnight cultures (Day 0), maximum fluorescence occurs at hour four in LB (Figure 8A), but does not reach maximum until 24 hours in both PBS and water. After three days in culture, however, all three cultures show a slight spike at four hours, and then another, greater increase, at 24 hours (Figure 9). After this maximum is reached, induction is maintained at that level in both LB and PBS (Figure 9A-B), whereas in water, this induction has a slight decrease (Figure 9C). In LB and PBS, the cultures that grew for three days before induction had greater fluorescence than those that were induced immediately (Figure 11). This could be due to the cells lying dormant and being stimulated by the addition of arabinose, which is a type of sugar, therefore creating a nutrients source (Figure 11). Opposite of this, in water, induction was not maintained as well in the day three cultures as they were in the day zero cultures (Figure 8C, Figure 9C). Looking specifically at the induced AraC circuit in all cultures, at day three induction, AraC fluorescence has much greater separation from the other circuits than that of day zero induction. Across all experimental environments, the positive controls show constant fluorescence and the negative controls show no fluorescence (Figure 9).

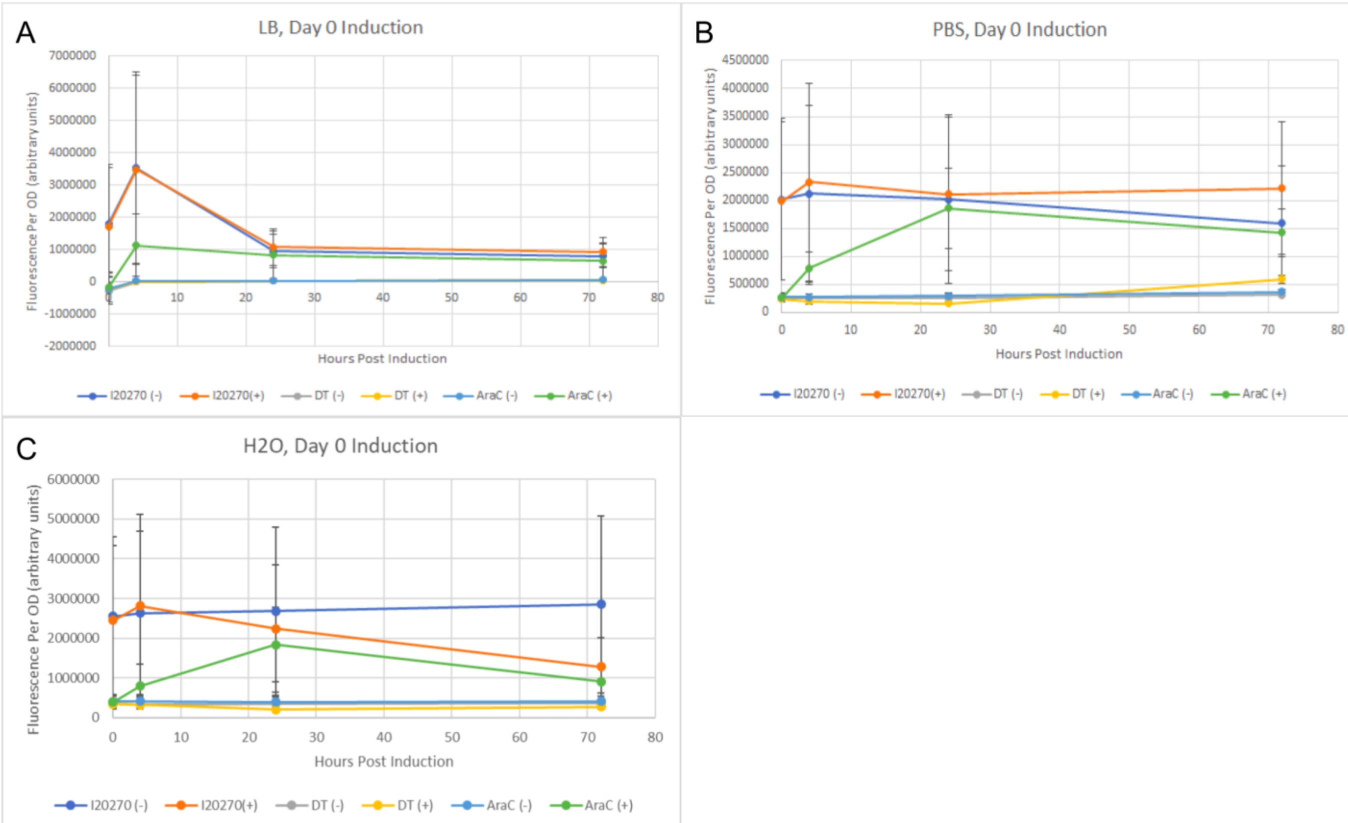

Figure 8: Fluorescence per OD measurements for day zero induction; A. LB culture, B. PBS culture, C. water culture. Three replicates of each experimental condition was performed. Error bars represent the standard error of the mean (+/- SEM) of the three experiments for each data point.

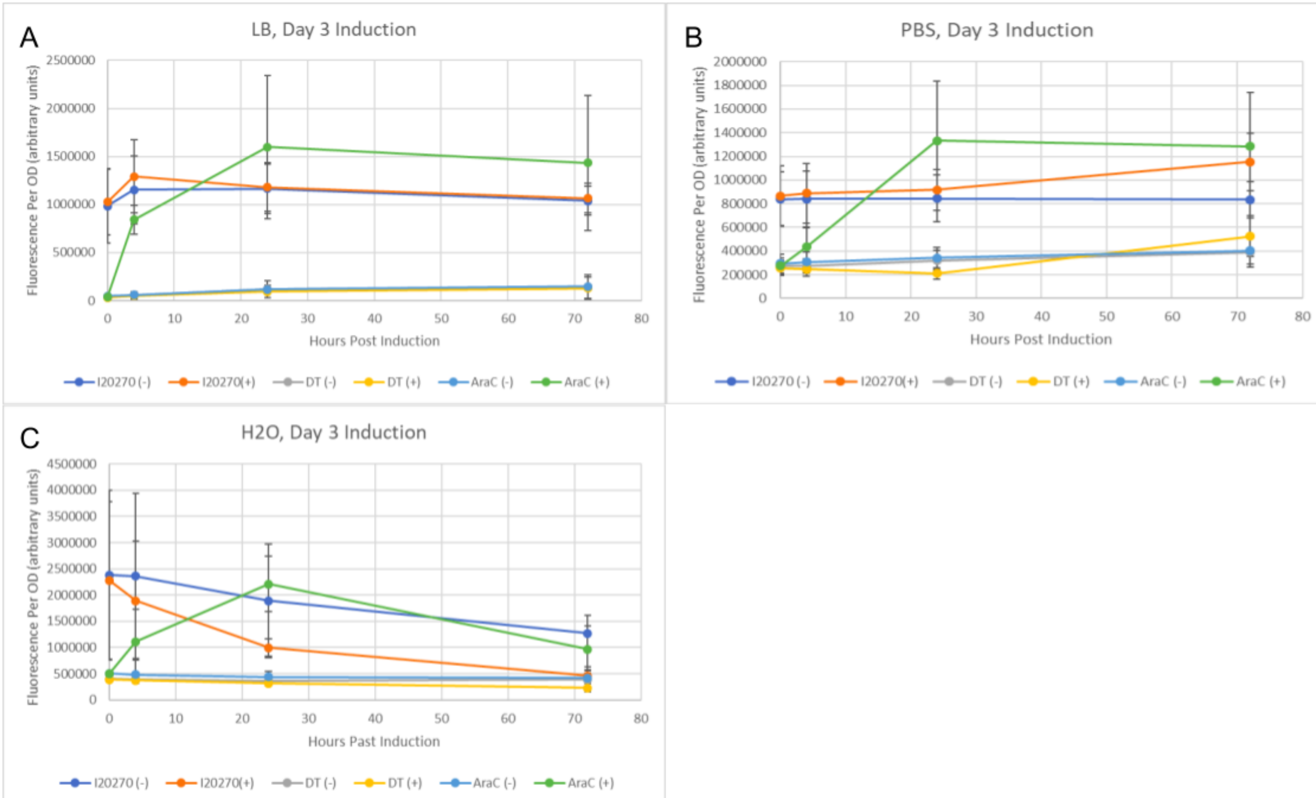

Figure 9: Fluorescence per OD measurements for day three induction; A. LB culture, B. PBS culture, C. water culture. Three replicates of each experimental condition was performed. Error bars represent the standard error of the mean (+/- SEM) of the three experiments for each data point.

The cultures that were induced after seven days of shaking did not follow the same patterns as the day zero and day three cultures. Unlike the day zero and day three cultures, all day seven cultures spiked after 24 hours post induction. The fluorescence of the AraC circuit also showed a much greater intensity than the positive controls in the day seven LB and PBS cultures, which was not observed in the zero and three day experiments (Figure 10A-B. This amount of separation was not seen in the day zero and three cultures. In the day seven water cultures, the fluorescence of all circuits remained constant, with slight decreases in the induced positive and negative controls (Figure 10C). These results show that the arabinose induction in these samples is no longer efficient. The induced AraC circuit is the only that exhibits an increase in fluorescence, again spiking at 24 hours, with a steep decrease thereafter (Figure 10C).

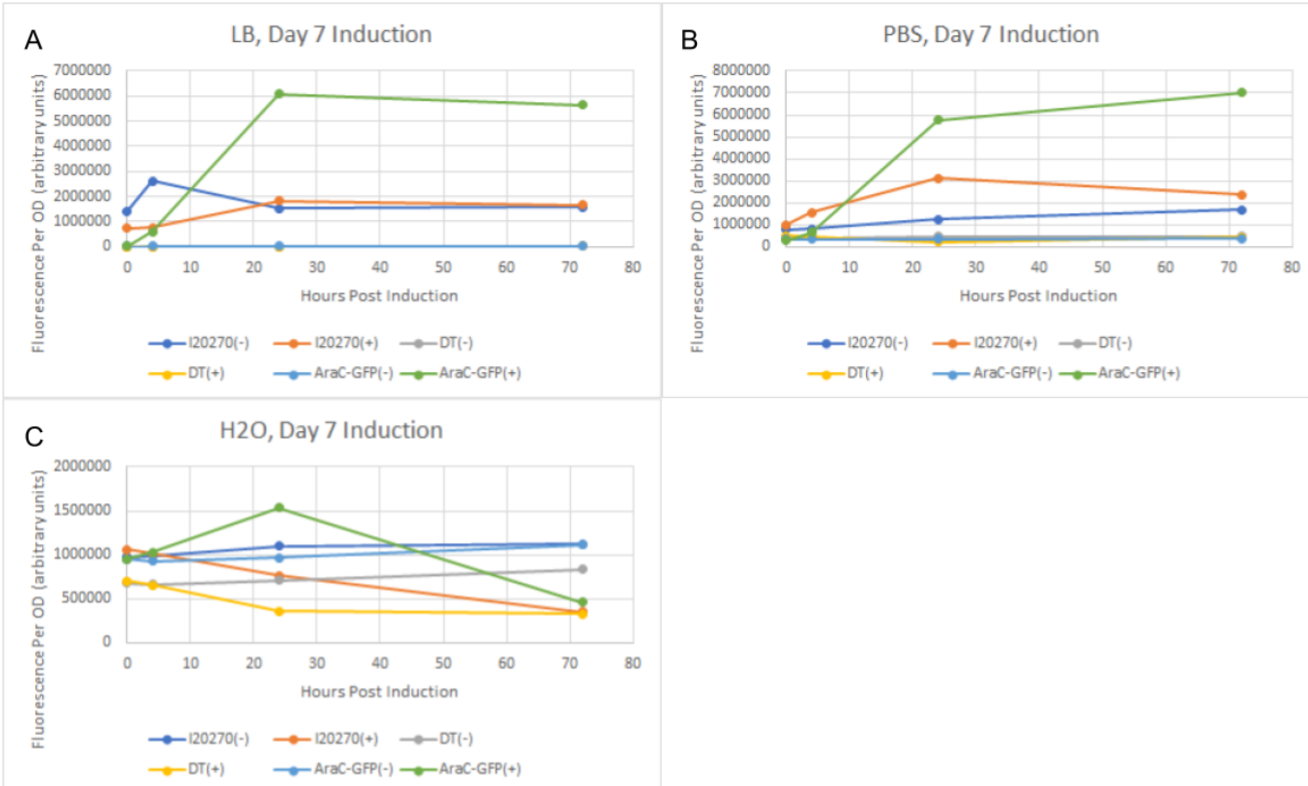

Figure 10: Fluorescence per OD measurements for day seven induction; A. LB culture, B. PBS culture, C. water culture. Three replicates of each experimental condition was performed. Error bars represent the standard error of the mean (+/- SEM) of the three experiments for each data point.

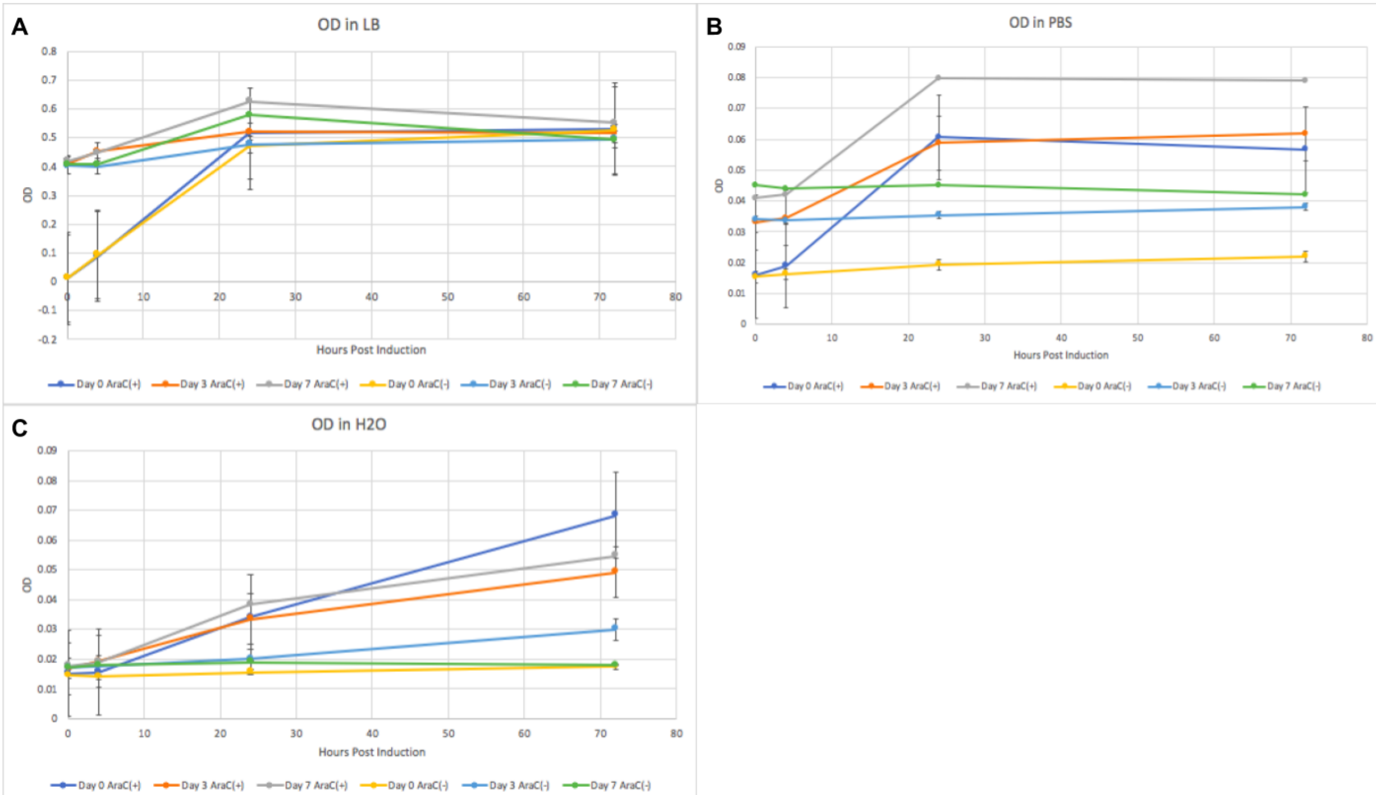

Figure 11: Analysis of OD in A. LB, B. PBS, and C. H2O. Three replicates of each experimental condition was performed. Error bars represent the standard error of the mean (+/- SEM) of the three experiments for each data point.

Arabinose is a monosaccharide, and while *E. coli* prefer glucose to other sugars, they can metabolize arabinose (Desai & Rao, 2010). In order to examine whether *E. coli* in nutrient limited conditions were metabolizing the arabinose for growth, we plotted the optical density (OD) measurements for the uninduced and induced cultures expressing the AraC-GFP plasmids under each of our experimental conditions. In all of the PBS and water cultures that have arabinose, the cells grow once the arabinose is added (Figure 11B-C). In the cultures that were not induced, no additional growth is observed. This shows that the cells are able to grow and can use the arabinose to facilitate the production of the GFP. In LB; however, the cultures have already reached a stationary phase, and the addition of arabinose does not confer any additional growth advantage. All cultures, whether induced or not, follow the same growth pattern (Figure 11A).

Discussion

Biosensor Cloning

Based on the unsuccessful attempts to clone the LacI-LacI circuit, it can be concluded that there were unanticipated mutations in either the inserts or the vector used. The inability to get clean digest patterns also supports this conclusion. These mutations affected the ability to perform diagnostic digests as well as led to difficulties with cloning. It should also be noted that some colonies looked red on the IPTG positive plate as well as the IPTG negative plate. This suggests that the fluorescent protein, mScarlet was present; however, even in the absence of the inducer, expression still occurred. Ultimately, the Lac promoter was not regulating mScarlet properly.

Induction Capacity

The data gathered above shows that in environments with limited resources, induction capacity of bacterial sensors decreases. At day zero induction in LB, the maximum fluorescence is seen at four hours post induction. This is because LB is a nutrient rich environment where bacteria thrive, therefore, induction happens rapidly. In both PBS and water, this spike is not observed until 24 hours post induction because they are lacking in nutrients causing the bacteria to have a slower response when induced. At day three induction, all three cultures had a small spike at four hours before reaching their maximum fluorescence at 24 hours. This data shows that during the three days of shaking, the bacteria use up some of the nutrients in their environment; therefore, they are not robust enough to reach their full potential after only four hours, and need a longer amount of time to be fully induced. This same pattern is seen with induction occurring after seven days. In LB and PBS, there is still a great amount of fluorescence and significant induction; however in water, induction is not as strong, there is a drop in the constitutive GFP, and there is overall less predictability. This is expected as there are no nutrients in water and the bacteria have not been growing (Figure 11). PBS; however, is more capable of maintaining inducibility as it does contain salts and other molecules that create a more favorable environment for the bacteria. This gives the PBS a buffering capacity that the water lacks. Ultimately this data reveals that even after a week in an environment with limited resources, bacterial sensors are still capable of induction.

Looking specifically at the behavior of the OD in each environment: LB, PBS, and water, we can understand how the cells are reacting. While it was expected that the decrease in induction capacity and fluorescence was due to the lack of environmental nutrients, that is not the case. Based on the data collected, it was observed that in LB both induced and uninduced circuits stopped growing, while the opposite occurred in PBS and water. In both PBS and water, the induced circuits continue to grow while the uninduced do not. It can then be concluded that, once induced, the arabinose is used as a carbon source and metabolized, allowing the cells to grow even in low nutrient environments.

The information gathered from this experiment shows that the induced cells were stimulated after the addition of arabinose, while the cells that were not induced with arabinose seemed to be in a dormant state. In the future this experiment could be replicated using a circuit and induction signal which has no nutritional qualities, such as heavy metals like arsenic or lead. This investigation would reveal whether dormant cells can induce a genetic circuit under these conditions. This could then reveal the true induction capacity of cells that have been kept in low nutrient environments.

References

Andrei Medvedovici, Florin Albu & Victor David (2010) HANDLING DRAWBACKS OF MASS SPECTROMETRIC DETECTION COUPLED TO LIQUID CHROMATOGRAPHY IN BIOANALYSIS, Journal of Liquid Chromatography & Related Technologies, 33:9-12, 1255-1286, DOI: 10.1080/10826076.2010.484375

Angenlini, D. J., Biggs, T. D., & Maughan, M. N. (2019). Evaluation of a lateral flow immunoassay for the detection of the synthetic opioid fentanyl. Forensic Science International, 300, 75–81. DOI: 10.1016/j.forsciint.2019.04.019

Bick, M. J., Greisen, P. J., Morey, K. J., Antunes, M. S., La, D., Sankaran, B., … Baker, D. (2017). Computational design of environmental sensors for the potent opioid fentanyl. eLife 2017;6:e28909 DOI: 10.7554/eLife.28909

Chan, C. T. Y., Lee, J. W., Cameron, D. E., Bashor, C. J., & Collins, J. J. (2015). Deadman' and 'Passcode' microbial kill switches for bacterial containment. *Nature Chemical Biology*, *12*, 82–86. DOI: 10.1038/nchembio.1979

Desai, T. A., & Rao, C. V. (2010). Regulation of Arabinose and Xylose Metabolism in Escherichia coli. Applied and Environmental Microbiology, 76 (5) 1524-1532; DOI: 10.1128/AEM.01970-09

Fentanyl (Rx). (2019, October 11). Retrieved April 16, 2020, from https://reference.medscape.com/drug/sublimaze-fentanyl-343311

Gandhi, S et al. "Recent advances in immunosensor for narcotic drug detection." *BioImpacts : BI* vol. 5,4 (2015): 207-13. DOI:10.15171/bi.2015.30

Goromaru T, Matsuura H, Yoshimura N, et al. Identification and quantitative determination of fentanyl metabolites in patients by gas chromatography--mass spectrometry. Anesthesiology. 1984 Jul;61(1):73-77.

Gushgari AJ, Venkatesan AK, Chen J, Steele JC, Halden RU. (2019) Long-term tracking of opioid consumption in two United States cities using wastewater-based epidemiology approach.Water Res. 2019 Sep 15;161:171-180. DOI: 10.1016/j.watres.2019.06.003

Harvard Health Publishing. (2011, June). Drugs in the water. Retrieved from https://www.health.harvard.edu/newsletter_article/drugs-in-the-water

Kawamura, A., & Miyata, T. (2016). Biosensors. Biomaterials Nanoarchitectonic. 157-176. DOI: 10.1016/B978-0-323-37127-8.00010-8

Klenkar, G., Liedberg, B. (2008). A microarray chip for label-free detection of narcotics. *Anal Bioanal Chem* 391, 1679–1688 (2008). DOI: 10.1007/s00216-008-1839-9

Liao, C. H., & Shollenberger, L. M. (2003). Survivability and long-term preservation of bacteria in water and in phosphate-buffered saline. Letters in Applied Microbiology 37, 45–50. DOI: 10.1046/j.1472-765X.2003.01345.x

Martin, S., Massa, V., Miller, H., & Reilly, S. (2018). *When Life Gives You Lyme: Investigating Repressors Important in the Transmission of Lyme Disease*. Retrieved from https://web.wpi.edu/Pubs/E-project/Available/E-project-042518-123455/unrestricted/When_Life_Gives_You_Lyme.pdf

Miller, S. G. (2018, May 25). Seattle Mussels Test Positive for Opioids. Retrieved from https://www.livescience.com/62667-puget-sound-mussels-opioids.html

National Institute on Drug Abuse. (2019, February). Fentanyl. Retrieved March 30, 2020, from https://www.drugabuse.gov/publications/drugfacts/fentanyl

National Institute on Drug Abuse. (2020, February 20). Opioid Overdose Crisis. Retrieved March 30, 2020, from https://www.drugabuse.gov/drugs-abuse/opioids/opioid-overdose-crisis

Opioid addiction, deaths, and treatment: The latest analysis of the data. (2019, May 20). Retrieved from https://usafacts.org/articles/opioid-addiction-deaths-and-treatment-latest-analysis-data/?utm_source=google&utm_medium=cpc&utm_campaign=healthcare&gclid=Cj0KCQiAqNPyBRCjARIsAKA-WFzZZD9lzE8OkAikTp07BcYz35t8DIHxBQwlaUczgcMNKIaoWcNJolcaAquFEALw_wcB

Suzuki, J., & El-Haddad, S. (2017). A review: Fentanyl and non-pharmaceutical fentanyls. Drug and Alcohol Dependence, 171, 107–116. DOI: 10.1016/j.drugalcdep.2016.11.033

Synthetic Opioid Overdose Data. (2020, March 19). Retrieved April 16, 2020, from https://www.cdc.gov/drugoverdose/data/fentanyl.html

Taylor, A. A. (2019, April 17). As more opioids go down the drain, scientists are tracking them in the environment. Retrieved from https://cen.acs.org/environment/water/opioids-down-drain-scientists-tracking/97/i16

The Truth About Fentanyl. (n.d.). Retrieved April 16, 2020, from https://www.drugfreeworld.org/newsletter/issue13/the-truth-about-fentanyl.html

Appendices

Appendix A: Sequences of Constructed Plasmids

Sequence 1. LacI ESM:

TTGCTGATTGGCGTTGCCACCTCCAGTCTGGCCCTGCACGCGCCGTCGCAAATTGTC
GCGGCGATTAAATCTCGCGCCGATCAACTGGGTGCCAGCGTGGTGGTGTCGATGGTA
GAACGAAGCGGCGTCGAAGCCTGTAAAGCGGCGGTGCACAATCTTCTCGCGCAACG
CGTCAGTGGGCTGATCATTAACTATCCGCTGGATGACCAGGATGCCATTGCTGTGGA
AGCTGCCTGCACTAATGTTCCGGCGTTATTTCTTGATGTCTCTGACCAGACACCCATC
AACAGTATTATTTTCTCCCATGAAGACGGTACGCGACTGGGCGTGGAGCATCTGGTC
GCATTGGGTCACCAGCAAATCGCGCTGTTAGCGGGCCCATTAAGTTCTGTCTCGGCG
CGTCTGCGTCTGGCTGGCTGGCATAAATATCTCACTCGCAATCAAATTCAGCCGATA
GCGGAACGGGAAGGCGACTGGAGTGCCATGTCCGGTTTTCAACAAACCATGCAAAT
GCTGAATGAGGGCATCGTTCCCACTGCGATGCTGGTTGCCAACGATCAGATGGCGCT
GGGCGCAATGCGCGCCATTACCGAGTCCGGGCTGCGCGTTGGTGCGGATATCTCGGT
AGTGGGATACGACGATACCGAAGACAGCTCATGTTATATCCCGCCGTTAACCACCAT
CAAACAGGATTTTCGCCTGCTGGGGCAAACCAGCGTGGACCGCTTGCTGCAACTCTC
TCAGGGCCAGGCGGTGAAGGGCAATCAGCTGTTGCCCGTCTCACTGGTGAAAAGAA
AAACCACCCTGGCGCCCAATACGCAAACCGCCTCTCCCCGCGCGTTGGCCGATTCAT
TAATGCAGCTGGCACGACAGGTTTCCCGACTGGAAAGCGGGCAGTGA

Sequence 2. LacI DRM:

ATGAAACCAGTAACGTTATACGATGTCGCAGAGTATGCCGGTGTCTCTTATCAGACC
GTTTCCCGCGTGGTGAACCAGGCCAGCCACGTTTCTGCGAAAACGCGGGAAAAAGT
GGAAGCGGCG

Sequence 3. GalR ESM:

AAACGGTCGGTCTGGTCGTTGGTGATGTTTCCGATCCGTTTTTCGGTGCAATGGTGA
AAGCGGTCGAACAGGTGGCTTATCACACCGGTAATTTTTTATTGATTGGCAACGGTT
ACCACAACGAACAAAAAGAGCGTCAGGCCATTGAGCAACTGATCCGCCATCGCTGT

GCTGCGTTGGTCGTCCATGCCAAAATGATCCCGGATGCTGATTTAGCCTCATTAATG
AAACAAATGCCCGGTATGGTGCTGATCAACCGTATCCTGCCTGGCTTTGAAAACCGT
TGTATTGCTCTGGACGATCGTTACGGTGCCTGGCTGGCAACGCGTCATTTAATTCAG
CAAGGTCATACCCGCATTGGTTATCTGTGCTCTAACCACTCTATTTCTGACGCCGAA
GATCGTCTGCAAGGGTATTACGATGCCCTTGCTGAAAGTGGTATTGCGGCCAATGAC
CGGCTGGTGACATTTGGCGAACCAGACGAAAGCGGCGGCGAACAGGCAATGACCG
AGCTTTTGGGACGAGGAAGAAATTTCACTGCGGTAGCCTGTTATAACGATTCAATGG
CGGCGGGTGCGATGGGCGTTCTCAATGATAATGGTATTGATGTACCGGGTGAGATTT
CGTTAATTGGCTTTGATGATGTGCTGGTGTCACGCTATGTGCGTCCGCGCCTGACCA
CCGTGCGTTACCCAATCGTGACGATGGCGACCCAGGCTGCCGAACTGGCTTTGGCGC
TGGCGGATAATCGCCCTCTCCCGGAAATCACTAATGTCTTTAGTCCGACGCTGGTAC
GTCGTCATTCAGTGTCAACTCCGTCGCTGGAGGCAAGTCATCATGCAACCAGCGACT
AA

Sequence 4. 2QZ3:
ATGGCATCTACTGACTACTGGCAGAATTGGACAGATGGTGGAGGGATCGTGAATGC
TGTCAATGGCTCGGGCGGAAACTATTCGGTTAATTGGTCGAATACGGGAAACTTTGT
TGTCGGGAAAGGTTGGACTACGGGTTCACCCTTCCGCACCATCAACTACAACGCGG
GTGTCTGGGCACCAAATGGAAACGGTTACTTAACCCTGTACGGGTGGACGCGCTCGC
CATTAATCGAGTATTACGTTGTCGATAGTTGGGGCACCTACCGCCCCACGGGTACCT
ATAAGGGGACTGTGAAGTCCGATGGGGGCACCTATGACATTTATACAACAACACGC
TACAATGCCCCGAGCATCGATGGAGATCGCACTACTTTCACGCAGTACTGGTCTGTA
CGTCAGTCGAAACGTCCTACCGGCTCAAATGCAACAATCACCTTTAGTAACCACGTT
AATGCTTGGAAGTCTCATGGCATGAATCTTGGATCGAATTGGGCTTATCAAGTCATG
GCTACTGCTGGTTATCAAAGTTCGGGCAGTTCGAATGTAACAGTTTGG

Sequence 5. mScarlet:

ATGGTGAGCAAGGGCGAGGCAGTGATCAAGGAGTTCATGCGGTTCAAGGTGCACAT
GGAGGGCTCCATGAACGGCCACGAGTTCGAGATCGAGGGCGAGGGCGAGGGCCGC
CCCTACGAGGGCACCCAGACCGCCAAGCTGAAGGTGACCAAGGGTGGCCCCCTGCC

CTTCTCCTGGGACATCCTGTCCCCTCAGTTCATGTACGGCTCCAGGGCCTTCATCAAG
CACCCCGCCGACATCCCCGACTACTATAAGCAGTCCTTCCCCGAGGGCTTCAAGTGG
GAGCGCGTGATGAACTTCGAGGACGGCGGCGCCGTGACCGTGACCCAGGACACCTC
CCTGGAGGACGGCACCCTGATCTACAAGGTGAAGCTCCGCGGCACCAACTTCCCTCC
TGACGGCCCCGTAATGCAGAAGAAGACAATGGGCTGGGAAGCGTCCACCGAGCGGT
TGTACCCCGAGGACGGCGTGCTGAAGGGCGACATTAAGATGGCCCTGCGCCTGAAG
GACGGCGGCCGCTACCTGGCGGACTTCAAGACCACCTACAAGGCCAAGAAGCCCGT
GCAGATGCCCGGCGCCTACAACGTCGACCGCAAGTTGGACATCACCTCCCACAACG
AGGACTACACCGTGGTGGAACAGTACGAACGCTCCGAGGGCCGCCACTCCACCGGC
GGCATGGACGAGCTGTACAAG

Appendix B: Plate Map

The plate map below correlates to the raw data in Appendix C for trials 2 and 3 and the single 7 day trial. Trial 1 has the same organization, just without the addition of the water column, as water was not tested in the first trial.

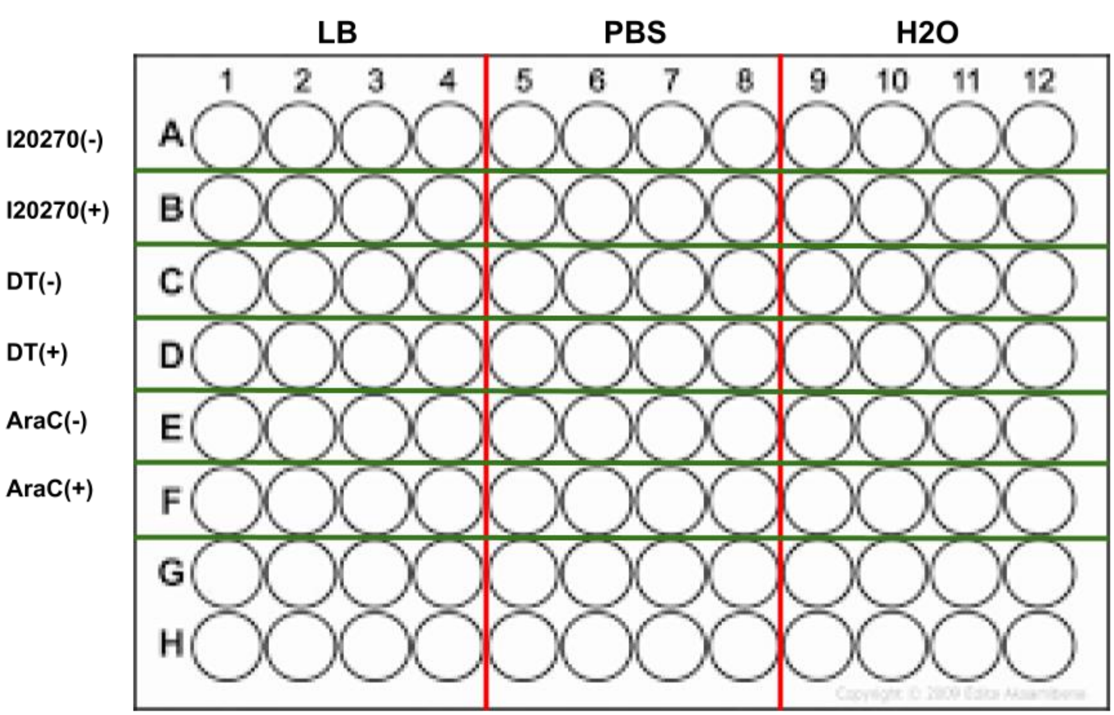

Appendix C: Plate Reader Raw Data

Trial 1:

Day 0 Time 0

A600 (Shell lab) (A)
-0.000

0.047	0.048	0.047	0.047	0.044	0.044	0.044	0.044
0.046	0.047	0.047	0.047	0.044	0.043	0.043	0.045
0.047	0.045	0.045	0.045	0.043	0.044	0.044	0.043
0.046	0.046	0.047	0.047	0.044	0.045	0.045	0.045
0.048	0.046	0.047	0.045	0.044	0.043	0.044	0.044
0.047	0.046	0.047	0.047	0.044	0.045	0.045	0.045

Fluorescein (1.0s) (Counts)
1019

51262	53920	51961	52698	12987	13084	12425	12853
52877	54089	53932	53068	12660	12623	12502	12957
46497	45436	45885	47055	6601	6959	6567	6691
46450	48101	48176	46505	6571	6861	6936	6873
46616	46575	47033	46913	6798	6767	6727	6931
47826	46557	48354	48016	6590	6878	7008	6964

Day 0 Time 4

A600 (Shell lab) (A)
-0.000

0.144	0.150	0.148	0.145	0.045	0.044	0.045	0.044
0.137	0.143	0.146	0.148	0.046	0.047	0.047	0.051
0.159	0.161	0.167	0.168	0.044	0.043	0.045	0.044
0.153	0.161	0.156	0.159	0.059	0.059	0.060	0.059
0.151	0.155	0.170	0.155	0.044	0.045	0.045	0.045
0.150	0.156	0.150	0.153	0.051	0.052	0.052	0.053

Fluorescein (1.0s) (Counts)
969

112909	117199	116835	116569	12807	12946	12992	12870
111206	113612	112252	113238	14560	15075	15015	16107
50287	50409	50516	50840	6926	7028	7173	6919
46995	49381	50040	48842	7438	7565	7563	7420
48940	49673	61946	50107	6932	7319	6954	7160
93927	97216	94603	95456	25180	25982	26453	26686

Day 0 Time 24

A600 (Shell lab) (A)
-0.000

0.514	0.527	0.548	0.527	0.045	0.045	0.046	0.046
0.515	0.527	0.537	0.538	0.089	0.091	0.092	0.095
0.512	0.531	0.538	0.527	0.050	0.052	0.052	0.051
0.541	0.551	0.562	0.561	0.110	0.112	0.113	0.115
0.501	0.518	0.521	0.509	0.063	0.049	0.050	0.048
0.525	0.525	0.549	0.551	0.109	0.115	0.113	0.114

Fluorescein (1.0s) (Counts)
1025

281173	288392	302670	290716	12744	12794	13102	13480
301066	310890	317702	315193	50403	52203	53745	55172
72852	76553	78412	76450	7450	7546	7642	7749
80372	83022	84046	84187	15895	16962	16789	16700
70975	75159	75499	73974	13314	7671	7846	7204
102956	103420	110358	110438	73636	79666	79394	78528

Day 0 Time 72

A600 (Shell lab) (A)
-0.000

0.626	0.637	0.641	0.646	0.047	0.046	0.047	0.046
0.629	0.655	0.657	0.659	0.085	0.084	0.086	0.088
0.627	0.632	0.641	0.647	0.060	0.059	0.060	0.060
0.626	0.655	0.649	0.654	0.098	0.097	0.094	0.100
0.613	0.635	0.635	0.630	0.058	0.057	0.057	0.057
0.626	0.643	0.641	0.646	0.092	0.092	0.091	0.094

Fluorescein (1.0s) (Counts)
1062

329233	337646	338771	342571	14590	14405	14399	14509
355649	376131	379212	375290	62489	62482	64004	63827
126986	128067	130756	130319	11889	12048	12134	12465
117566	126371	125232	124511	35273	36028	35413	36350
117531	123216	123795	122202	11411	11312	11177	11463
141672	148508	147746	148399	78733	80760	79220	81008

Day 3 Time 0

A600 (Shell lab) (A)
-0.000

0.450	0.455	0.461	0.457	0.048	0.048	0.048	0.047
0.445	0.460	0.455	0.460	0.048	0.048	0.048	0.049
0.475	0.481	0.479	0.472	0.069	0.069	0.069	0.069
0.506	0.489	0.492	0.493	0.063	0.063	0.063	0.064
0.463	0.480	0.472	0.478	0.064	0.063	0.063	0.063
0.466	0.485	0.486	0.481	0.065	0.066	0.065	0.066

Fluorescein (1.0s) (Counts)
1001

233538	237044	241651	240418	14200	14248	14058	14275
228648	237137	235469	236009	14815	14871	14915	14823
77782	77917	78541	78299	15863	16357	15841	15988
78574	78977	79297	78499	12491	12684	12723	12836
75564	78330	77792	77989	12937	13126	12778	13053
74416	78352	78101	76186	13131	13394	13090	13209

Day 3 Time 4

A600 (Shell lab) (A)
-0.000

0.479	0.540	0.486	0.490	0.048	0.047	0.048	0.048
0.543	0.541	0.547	0.554	0.050	0.050	0.050	0.051
0.498	0.503	0.506	0.501	0.071	0.069	0.070	0.070
0.564	0.568	0.585	0.585	0.067	0.067	0.068	0.069
0.554	0.518	0.511	0.506	0.065	0.063	0.064	0.063
0.548	0.553	0.565	0.554	0.068	0.068	0.068	0.070

Fluorescein (1.0s) (Counts)
949

281115	319854	288387	291816	14341	14633	14175	14694
308683	308427	308461	311008	16039	16374	16330	16536
96267	98589	99824	98518	16845	17151	16707	17076
102293	106582	108219	105710	13219	13451	13693	13751
100675	100278	98913	99340	14079	13839	13885	14053
368544	379459	382524	375078	32396	33266	33026	33395

Day 3 Time 24

A600 (Shell lab) (A)
-0.000

0.555	0.576	0.573	0.570	0.049	0.050	0.050	0.050
0.596	0.621	0.610	0.630	0.090	0.089	0.090	0.095
0.558	0.562	0.582	0.576	0.076	0.073	0.076	0.076
0.650	0.649	0.646	0.652	0.101	0.101	0.105	0.107
0.564	0.587	0.573	0.566	0.069	0.067	0.069	0.069
0.604	0.604	0.624	0.614	0.105	0.106	0.109	0.111

Fluorescein (1.0s) (Counts)
998

397464	411470	407056	410721	15504	16371	16403	16470
380156	399989	392965	409118	61920	62286	63923	67726
189666	193902	195197	201480	22682	22562	23438	24031
169003	174532	173260	175902	25022	25776	27259	26496
188474	199653	200512	196266	17890	18160	18563	19298
411516	414226	426381	421343	109478	110505	117282	117459

Day 3 Time 72

A600 (Shell lab) (A)
-0.000

0.554	0.563	0.566	0.576	0.052	0.052	0.052	0.051
0.646	0.664	0.669	0.678	0.079	0.078	0.080	0.081
0.561	0.587	0.577	0.590	0.081	0.080	0.081	0.080
0.657	0.674	0.687	0.675	0.091	0.092	0.091	0.094
0.558	0.587	0.582	0.582	0.074	0.073	0.073	0.073
0.657	0.664	0.675	0.680	0.094	0.093	0.093	0.094

Fluorescein (1.0s) (Counts)
951

438975	457356	457521	473074	18409	17982	18156	17880
428788	445608	449676	457638	78966	78362	81813	82233
258032	273795	272599	281113	34851	35520	34811	34517
232911	243038	248193	243570	49419	50871	51137	50987
264410	284766	277916	281170	28071	28297	27276	28748
358618	372578	381203	379969	111029	112088	111588	111002

Trial 2:

Day 0 Time 0

A600 (Shell lab) (A)
-0.000

0.028	0.036	0.028	0.029	0.031	0.030	0.029	0.029	0.028	0.029	0.029	0.029
0.045	0.043	0.044	0.044	0.043	0.043	0.043	0.044	0.042	0.042	0.043	0.043
0.046	0.044	0.044	0.044	0.043	0.044	0.044	0.044	0.042	0.043	0.042	0.042
0.044	0.043	0.044	0.043	0.043	0.043	0.043	0.043	0.043	0.043	0.043	0.045
0.042	0.042	0.042	0.042	0.043	0.043	0.043	0.043	0.042	0.043	0.043	0.042
0.045	0.045	0.045	0.045	0.048	0.047	0.046	0.047	0.046	0.046	0.046	0.046
0.045	0.045	0.044	0.044	0.047	0.047	0.046	0.047	0.047	0.047	0.047	0.047

Fluorescein (1.0s) (Counts)
975

3790	4514	3723	3924	3984	4024	3907	3790	3699	4164	3819	4009
9226	9348	9657	9637	11593	11682	11937	12153	11125	11428	11630	12188
9579	9422	9340	9460	11537	12088	12224	12396	11554	12065	11794	12171
5322	5415	5413	5535	6671	6785	6713	6708	6891	6892	6954	7443
7955	8052	7886	8017	6754	6625	6710	6875	6815	6919	7223	7234
5401	5539	5404	5446	7894	7793	7772	7572	7931	7952	7913	8215
6381	6312	6377	6195	7744	7626	7562	7733	8151	8246	8341	8508

Day 0 Time 4

A600 (Shell lab) (A)
-0.000

0.028	0.029	0.028	0.029	0.028	0.029	0.028	0.029	0.029	0.029	0.029	0.029
0.116	0.114	0.113	0.118	0.044	0.044	0.043	0.046	0.043	0.043	0.043	0.043
0.115	0.111	0.111	0.111	0.044	0.044	0.044	0.045	0.044	0.044	0.044	0.052
0.120	0.116	0.118	0.116	0.043	0.043	0.043	0.043	0.043	0.043	0.043	0.043
0.120	0.115	0.116	0.114	0.045	0.044	0.044	0.045	0.043	0.044	0.044	0.044
0.135	0.128	0.129	0.127	0.047	0.047	0.047	0.047	0.046	0.046	0.046	0.046
0.133	0.129	0.130	0.129	0.048	0.048	0.048	0.048	0.048	0.048	0.048	0.048

Fluorescein (1.0s) (Counts)
966

3641	4043	3710	3692	3867	3588	4014	3845	4004	4177	3819	4158
55748	55975	55319	57761	11609	12075	11847	11818	11717	12295	11875	12274
54611	53004	51655	52780	11824	12074	11792	12657	12158	12676	12402	13737
5569	5786	5645	5917	6947	6903	6933	7197	6822	7244	7181	7535
7094	7119	6852	7040	7073	7013	6911	7095	7182	7303	7333	7551
7253	7337	7254	7462	7689	8060	8045	7887	8153	8124	8201	8469
6930	7130	6916	6931	7876	8103	8189	8188	8599	8451	8828	8983

Day 0 Time 24

A600 (Shell lab) (A)
-0.000

0.028	0.028	0.029	0.029	0.029	0.029	0.029	0.030	0.028	0.029	0.029	0.029
0.564	0.541	0.558	0.551	0.045	0.044	0.045	0.045	0.043	0.044	0.044	0.044
0.565	0.546	0.556	0.545	0.073	0.076	0.076	0.076	0.050	0.050	0.052	0.050
0.546	0.529	0.531	0.532	0.044	0.044	0.044	0.045	0.043	0.043	0.045	0.045
0.591	0.575	0.577	0.578	0.073	0.073	0.072	0.076	0.052	0.054	0.055	0.054
0.544	0.533	0.530	0.529	0.048	0.049	0.048	0.049	0.046	0.047	0.048	0.047
0.574	0.548	0.552	0.545	0.074	0.074	0.074	0.075	0.053	0.054	0.055	0.054

Fluorescein (1.0s) (Counts)
986

4189	3871	3979	4091	4084	3753	4191	4169	3878	4039	3955	4021
236006	223049	229731	223656	11820	11974	12427	12405	12228	12193	12648	13192
258057	251920	251116	247140	34503	37987	38365	37340	17820	17668	17907	18008
9323	9234	9214	9221	7222	7451	7808	7761	7513	7528	7972	8143
9331	9187	9000	9118	11153	11133	11352	11542	8706	8881	9162	9268
11147	11243	11097	10907	8539	8964	8765	8761	8728	9047	9020	8843
55103	52762	52545	51822	67674	68071	68520	68510	26667	27035	27049	27115

Day 0 Time 72

A600 (Shell lab) (A)
-0.000

0.028	0.028	0.029	0.029	0.029	0.029	0.029	0.029	0.028	0.029	0.029	0.029
0.576	0.566	0.564	0.563	0.046	0.046	0.046	0.047	0.044	0.044	0.045	0.045
0.626	0.606	0.620	0.608	0.077	0.079	0.079	0.078	0.060	0.061	0.062	0.061
0.553	0.545	0.548	0.540	0.046	0.046	0.046	0.047	0.048	0.044	0.045	0.045
0.589	0.566	0.569	0.568	0.074	0.076	0.074	0.076	0.061	0.061	0.061	0.061
0.556	0.549	0.548	0.543	0.049	0.050	0.049	0.050	0.047	0.047	0.048	0.048
0.601	0.587	0.585	0.580	0.076	0.074	0.074	0.075	0.059	0.060	0.061	0.060

Fluorescein (1.0s) (Counts)
1005

3832	3771	3915	3790	4114	3757	4054	3966	3891	4307	3872	3916
208211	205370	201892	201203	13433	13495	14301	14144	13338	13568	14407	14255
242708	237321	240331	236153	51306	55363	56203	52885	20928	21994	21402	21859
13899	13910	13821	13892	9256	9196	9124	9511	8702	9266	9060	9521
18316	17871	17679	17519	29904	31835	30700	31052	10831	10727	10631	10758
14000	13931	14136	14078	11913	12129	11999	12205	11305	11565	11137	11594
32143	32309	31319	31328	41415	42061	41850	41979	33555	33906	34715	34102

Day 3 Time 0

A600 (Shell lab) (A)
-0.000

0.028	0.029	0.028	0.028	0.028	0.029	0.029	0.029	0.028	0.029	0.029	0.029
0.412	0.408	0.406	0.406	0.044	0.045	0.046	0.046	0.042	0.042	0.043	0.043
0.431	0.412	0.415	0.431	0.045	0.045	0.046	0.046	0.042	0.042	0.042	0.042
0.518	0.512	0.521	0.513	0.044	0.046	0.044	0.045	0.042	0.042	0.042	0.042
0.431	0.423	0.438	0.419	0.045	0.045	0.045	0.046	0.040	0.042	0.041	0.041
0.418	0.406	0.405	0.402	0.051	0.051	0.051	0.051	0.047	0.047	0.048	0.047
0.471	0.461	0.458	0.454	0.047	0.047	0.047	0.048	0.046	0.047	0.048	0.048

Fluorescein (1.0s) (Counts)
948

4003	3770	3795	3859	3972	3869	3932	3892	3823	4215	3995	4078
294811	292394	283961	288329	14507	15101	15853	15593	14217	14345	15107	15377
341045	314363	313496	389258	14451	14746	15521	15021	14144	14537	14134	14896
22371	22369	22575	22810	9919	9937	10141	10006	9783	9892	9798	10147
11806	11893	12215	11890	9997	9904	10020	10188	9344	9503	9555	9784
21254	20841	20564	20419	13750	14208	14067	14176	13106	13604	13707	13515
19244	19294	18907	18805	11060	11497	11672	11413	13024	13295	13913	13976

Day 3 Time 4

A600 (Shell lab) (A)
-0.000

0.028	0.029	0.029	0.028	0.028	0.029	0.029	0.029	0.028	0.029	0.029	0.029
0.418	0.406	0.403	0.403	0.045	0.045	0.047	0.046	0.042	0.042	0.044	0.043
0.425	0.412	0.412	0.411	0.045	0.045	0.045	0.046	0.043	0.043	0.043	0.043
0.547	0.539	0.542	0.529	0.044	0.045	0.045	0.047	0.042	0.042	0.042	0.042
0.445	0.436	0.441	0.435	0.046	0.046	0.046	0.046	0.041	0.042	0.042	0.041
0.442	0.416	0.425	0.452	0.051	0.051	0.051	0.051	0.047	0.047	0.048	0.047
0.502	0.483	0.491	0.486	0.047	0.047	0.047	0.048	0.050	0.047	0.048	0.048

Fluorescein (1.0s) (Counts)
929

3936	3787	4031	3993	4291	4119	4114	4253	3905	4146	3945	4039
445835	436330	430814	431824	15172	15230	16167	15796	14804	14900	15698	15125
538443	530253	515684	529434	15342	15696	15435	15650	14426	14797	14858	15109
21303	21303	21062	21008	9988	10013	10034	9943	9636	10025	10133	10412
14317	14512	14250	14272	10157	10042	10261	10219	9361	9676	9546	9894
20098	19377	19426	23166	14343	14549	14519	14370	13527	14070	13953	13989
541284	523962	532102	525979	11593	11733	11842	11638	13415	13430	13821	14169

Day 3 Time 24

A600 (Shell lab) (A)
-0.000

0.028	0.028	0.029	0.028	0.028	0.029	0.029	0.029	0.028	0.029	0.029	0.029
0.487	0.478	0.481	0.471	0.044	0.045	0.045	0.045	0.042	0.042	0.043	0.043
0.535	0.533	0.530	0.520	0.071	0.070	0.070	0.072	0.046	0.046	0.047	0.047
0.518	0.514	0.517	0.504	0.044	0.045	0.044	0.045	0.042	0.042	0.042	0.042
0.476	0.477	0.485	0.475	0.072	0.073	0.073	0.074	0.045	0.046	0.046	0.046
0.515	0.506	0.507	0.504	0.050	0.050	0.050	0.050	0.046	0.047	0.047	0.047
0.591	0.579	0.579	0.571	0.051	0.051	0.051	0.052	0.049	0.050	0.050	0.051

Fluorescein (1.0s) (Counts)
1026

3785	3696	3921	3810	4017	3815	4145	3774	3991	4030	4021	4130
561779	557137	552127	545668	15333	15227	15705	15684	14852	15109	15164	15587
666096	672384	655402	647708	52885	53451	54098	54486	19047	19131	19470	19730
25985	25623	25386	25290	9886	10404	10408	10213	10151	10329	10215	10261
21324	21227	21464	21192	11555	11705	11764	11795	10112	10075	10243	10089
20802	20632	20464	20648	14355	14450	13873	14650	13508	14031	13689	13771
1738782	1708691	1702681	1672894	52070	52213	52678	53318	60101	61618	62072	66629

Day 3 Time 72

A600 (Shell lab) (A)
-0.000

0.028	0.028	0.029	0.029	0.029	0.029	0.029	0.029	0.028	0.029	0.029	0.029
0.506	0.492	0.506	0.502	0.045	0.045	0.045	0.046	0.042	0.042	0.044	0.042
0.545	0.539	0.534	0.536	0.076	0.076	0.076	0.079	0.058	0.059	0.059	0.059
0.510	0.503	0.505	0.506	0.044	0.045	0.045	0.045	0.042	0.042	0.042	0.042
0.492	0.632	0.477	0.472	0.071	0.071	0.071	0.073	0.058	0.058	0.059	0.060
0.517	0.527	0.520	0.520	0.050	0.051	0.051	0.051	0.047	0.047	0.048	0.047
0.550	0.527	0.535	0.526	0.069	0.069	0.069	0.070	0.062	0.064	0.064	0.064

Fluorescein (1.0s) (Counts)
983

3886	3842	3794	3745	3730	3976	3907	3948	3972	4243	4017	4113
544930	531744	544982	542191	15947	16316	16868	16790	16237	16464	17595	16821
624439	622732	602469	612196	63154	63761	64346	65054	20762	21089	20632	20944
13378	13296	19184	13323	10250	10348	10668	10758	11359	11471	11680	11883
11751	20971	11521	11691	31270	31827	31191	32049	13248	13438	13620	14037
17983	18657	18071	18202	14944	14919	14978	14381	15426	15829	15777	16010
1485077	1421787	1431082	1407397	76019	75465	76384	77290	52377	53307	54085	53657

Trial 3:

Day 0 Time 0

A600 (Shell lab) (A)
-0.000

0.028	0.029	0.028	0.028	0.028	0.028	0.028	0.029	0.029	0.029	0.029	0.029
0.038	0.038	0.038	0.038	0.043	0.042	0.042	0.042	0.040	0.041	0.041	0.041
0.037	0.039	0.041	0.039	0.042	0.042	0.042	0.042	0.041	0.041	0.041	0.041
0.040	0.040	0.040	0.040	0.042	0.042	0.041	0.042	0.039	0.040	0.039	0.039
0.037	0.038	0.038	0.039	0.042	0.042	0.042	0.042	0.039	0.040	0.040	0.040
0.040	0.040	0.042	0.040	0.043	0.043	0.042	0.043	0.040	0.040	0.040	0.040
0.038	0.038	0.038	0.038	0.044	0.043	0.042	0.043	0.041	0.040	0.041	0.040

Fluorescein (1.0s) (Counts)
1005

3493	3808	3680	3723	3705	3762	4006	3776	3825	3943	3800	4015
56428	54998	56779	58081	69846	72276	68766	71194	55969	61290	57435	59012
50635	67825	61837	64000	70473	69785	68752	70991	55259	55041	57209	55749
5194	5235	5342	5171	8692	8330	8411	8384	8868	9045	9100	9207
5255	5405	5441	5627	8379	8561	8364	8595	8895	8811	9107	9183
6664	6726	6634	6844	9779	9743	9672	9434	10047	10110	10455	10641
7469	7453	7734	7676	9892	9809	9884	9668	10326	10283	10647	10524

Day 0 Time 4

A600 (Shell lab) (A)
-0.000

0.028	0.028	0.028	0.029	0.028	0.029	0.029	0.029	0.029	0.029	0.029	0.029
0.057	0.056	0.057	0.056	0.041	0.041	0.041	0.041	0.041	0.042	0.042	0.042
0.056	0.054	0.055	0.056	0.044	0.047	0.045	0.046	0.042	0.042	0.043	0.043
0.089	0.089	0.089	0.087	0.042	0.042	0.042	0.042	0.040	0.040	0.040	0.040
0.090	0.088	0.090	0.086	0.045	0.044	0.045	0.045	0.041	0.042	0.042	0.043
0.088	0.085	0.084	0.084	0.043	0.044	0.044	0.043	0.040	0.040	0.040	0.041
0.082	0.080	0.080	0.079	0.044	0.043	0.044	0.043	0.041	0.041	0.041	0.041

Fluorescein (1.0s) (Counts)
1062

3562	3688	3790	3597	3873	3712	4173	4283	3926	3828	3682	3548
280074	262438	271640	265583	67057	70776	70533	68084	60869	65013	66904	64031
270720	250595	244714	257997	96766	107903	103408	102212	72700	74831	75932	74487
6402	6578	6234	6561	8267	8527	8377	8626	8478	8940	8860	8900
7568	7437	7493	7463	8358	8513	8579	8414	8942	9157	8979	9359
8195	8549	8191	8332	9698	9688	9677	10005	10227	10576	10196	10715
163244	164594	159908	161397	21278	21455	21861	21239	19705	20820	19882	19952

Day 0 Time 24

A600 (Shell lab) (A)
-0.000

0.028	0.028	0.028	0.029	0.031	0.029	0.029	0.029	0.028	0.029	0.029	0.029
0.514	0.494	0.497	0.496	0.042	0.043	0.043	0.043	0.043	0.043	0.044	0.044
0.520	0.502	0.511	0.500	0.086	0.088	0.087	0.089	0.074	0.074	0.075	0.076
0.471	0.454	0.463	0.443	0.043	0.043	0.041	0.043	0.040	0.040	0.041	0.041
0.516	0.500	0.496	0.492	0.094	0.088	0.089	0.089	0.073	0.073	0.073	0.074
0.471	0.455	0.456	0.460	0.045	0.045	0.043	0.043	0.041	0.041	0.041	0.041
0.557	0.546	0.546	0.539	0.082	0.082	0.081	0.083	0.070	0.071	0.072	0.072

Fluorescein (1.0s) (Counts)
994

3465	3661	3785	3706	3941	3757	4061	4214	3976	4227	3984	4053
969890	918252	918593	915931	69511	70434	70491	73931	71428	71085	76147	79480
1102815	1072738	1073748	1058299	279385	287501	285961	286465	178945	177871	183413	183196
15840	15582	15355	15304	8816	9038	8799	9103	9314	9423	9276	9431
13763	13808	13692	13870	13238	13693	13757	13879	13172	13129	13027	13125
15352	15018	15163	15430	10025	10334	10095	9884	10412	10541	10667	10909
1232688	1216197	1204444	1191300	174979	176480	178607	176656	120095	121925	123939	123051

Day 0 Time 72

A600 (Shell lab) (A)
-0.000

0.028	0.028	0.029	0.028	0.029	0.029	0.028	0.029	0.029	0.029	0.029	0.029
0.520	0.506	0.512	0.528	0.046	0.045	0.045	0.046	0.043	0.044	0.043	0.043
0.560	0.550	0.549	0.550	0.088	0.089	0.088	0.090	0.101	0.099	0.098	0.097
0.505	0.501	0.498	0.498	0.043	0.044	0.044	0.044	0.042	0.042	0.043	0.042
0.566	0.559	0.577	0.580	0.084	0.084	0.084	0.084	0.089	0.121	0.113	0.095
0.499	0.487	0.498	0.485	0.045	0.045	0.044	0.045	0.044	0.047	0.044	0.045
0.514	0.508	0.523	0.509	0.089	0.091	0.089	0.089	0.128	0.143	0.124	0.141

Fluorescein (1.0s) (Counts)
952

3492	3888	3679	3591	3789	3450	4047	3760	3976	4112	3887	4219
758923	741929	741229	783162	65902	65105	66979	66015	74962	76730	77701	77412
956038	950931	936084	939956	278735	284599	279880	279357	149131	144546	141904	140812
10349	10560	10304	10542	9400	9574	9586	9589	9512	9539	9634	9846
10789	10705	10971	11022	42867	43499	43567	42694	29190	29102	29149	29504
10281	10500	10182	10037	10609	10858	10801	10871	10652	10719	10914	10931
845747	836209	866297	832904	140865	142039	139905	138188	91107	96054	91300	96830

Day 3 Time 0

A600 (Shell lab) (A)
-0.000

0.028	0.029	0.028	0.028	0.028	0.029	0.029	0.029	0.029	0.029	0.029	0.029
0.424	0.412	0.418	0.411	0.071	0.071	0.071	0.074	0.044	0.044	0.045	0.044
0.502	0.494	0.486	0.515	0.071	0.072	0.072	0.070	0.045	0.045	0.045	0.045
0.447	0.449	0.434	0.429	0.070	0.068	0.068	0.070	0.044	0.044	0.044	0.044
0.455	0.441	0.441	0.437	0.070	0.071	0.071	0.072	0.043	0.044	0.044	0.044
0.431	0.418	0.419	0.416	0.072	0.072	0.072	0.073	0.043	0.043	0.043	0.044
0.467	0.449	0.456	0.456	0.073	0.072	0.072	0.072	0.043	0.043	0.044	0.044

Fluorescein (1.0s) (Counts)
945

3547	3935	3657	3484	3889	3660	4170	4116	3920	4214	4069	4090
689073	675549	672724	665457	58515	58563	58703	61048	66281	66645	67488	66695
808703	794923	773533	823783	62676	62347	62393	61062	64675	65833	66388	67224
7182	7504	7222	7129	10223	10266	10019	10170	9649	9933	9796	9762
7488	7828	7672	7379	9860	9919	10244	10119	8878	9012	8902	9096
10085	10042	9902	10004	11224	11337	11222	11687	11070	11324	11376	11641
7459	7332	7241	7383	11476	11444	11589	11392	11251	11208	11384	11343

Day 3 Time 4

A600 (Shell lab) (A)
-0.000

0.028	0.028	0.028	0.028	0.028	0.028	0.028	0.029	0.028	0.029	0.029	0.029
0.434	0.418	0.417	0.427	0.071	0.074	0.072	0.073	0.045	0.045	0.046	0.045
0.537	0.524	0.542	0.559	0.071	0.071	0.071	0.071	0.051	0.051	0.052	0.051
0.445	0.428	0.426	0.433	0.069	0.069	0.068	0.069	0.045	0.045	0.045	0.046
0.529	0.507	0.512	0.509	0.073	0.073	0.072	0.073	0.044	0.045	0.045	0.045
0.436	0.410	0.422	0.414	0.072	0.072	0.072	0.073	0.045	0.045	0.045	0.044
0.508	0.487	0.487	0.485	0.075	0.074	0.073	0.073	0.047	0.048	0.048	0.048

Fluorescein (1.0s) (Counts)
990

3609	3945	3684	3632	3889	3581	4111	4062	3800	3923	3727	3595
728188	695619	684580	705202	59589	62567	59769	62003	67954	68815	71071	69101
875583	852192	894653	1318098	62401	64354	63538	63181	69522	70936	72544	73098
10187	10076	10022	10201	10207	10065	10085	10177	9578	9561	9388	9564
9818	9674	9819	9610	10145	10020	10005	10050	8688	8722	8704	8922
10458	10023	10403	10209	11364	11493	11186	11601	10796	11004	10889	10945
310125	299646	294582	293347	11468	11490	11670	11615	35653	36957	36630	36837

Day 3 Time 24

A600 (Shell lab) (A)
-0.000

0.028	0.029	0.029	0.028	0.028	0.028	0.029	0.029	0.029	0.029	0.029	0.029
0.424	0.423	0.425	0.427	0.074	0.074	0.075	0.075	0.050	0.050	0.050	0.050
0.510	0.498	0.498	0.498	0.101	0.102	0.102	0.157	0.073	0.074	0.075	0.074
0.452	0.436	0.441	0.436	0.071	0.071	0.072	0.071	0.052	0.053	0.053	0.052
0.524	0.513	0.509	0.506	0.086	0.085	0.086	0.086	0.066	0.070	0.067	0.067
0.457	0.424	0.442	0.434	0.073	0.074	0.074	0.074	0.052	0.052	0.051	0.050
0.570	0.540	0.543	0.542	0.102	0.105	0.103	0.103	0.076	0.073	0.075	0.073

Fluorescein (1.0s) (Counts)
984

3563	3930	3537	3623	3625	3543	3871	3804	3704	3852	3630	3921
632925	628952	627616	630431	58936	58644	61431	60744	66417	67015	66838	67225
744409	732396	719513	724549	57424	58308	59190	48562	55091	56383	56902	56825
12521	12776	12393	12271	10075	10484	10644	10465	9820	9958	10182	10422
11500	11635	11454	11428	12259	12529	12956	12373	10256	26240	10479	10678
13696	13235	13593	13296	11624	11625	11775	11862	11488	11501	11381	11834
528361	502384	501050	502027	35380	36537	36294	36659	79184	80264	81973	80464

Day 3 Time 72

A600 (Shell lab) (A)
-0.000

0.028	0.029	0.028	0.029	0.029	0.029	0.029	0.029	0.029	0.029	0.029	0.029
0.477	0.470	0.473	0.465	0.077	0.077	0.078	0.078	0.063	0.067	0.064	0.064
0.522	0.503	0.510	0.507	0.106	0.107	0.106	0.108	0.102	0.095	0.103	0.124
0.471	0.458	0.464	0.456	0.073	0.074	0.074	0.075	0.066	0.066	0.067	0.067
0.530	0.512	0.506	0.510	0.091	0.092	0.092	0.094	0.096	0.099	0.100	0.105
0.494	0.474	0.469	0.474	0.076	0.076	0.075	0.076	0.068	0.072	0.069	0.070
0.557	0.542	0.540	0.538	0.108	0.110	0.109	0.111	0.092	0.090	0.093	0.094

Fluorescein (1.0s) (Counts)
993

3820	4131	3691	3800	3707	3655	4151	3780	3866	4172	3795	4272
561525	552516	547819	539678	57027	59326	59782	60715	60977	62587	62440	62401
615138	592071	594887	593220	56862	58055	58246	59086	31058	31422	32216	32549
15325	15800	15711	15376	10966	10875	11143	11317	11569	11767	12073	12289
7600	7406	7181	7490	15137	15392	15606	15768	14546	14653	14877	14786
11804	11606	11479	11331	11778	12075	12004	11903	12720	12985	12782	13143
453971	447394	440866	438680	34153	34631	34710	35070	36479	36304	36671	36971

Day 7 Time 0

A600 (Shell lab) (A)
-0.000

0.028	0.029	0.028	0.029	0.028	0.028	0.029	0.028	0.029	0.029	0.030	0.029
0.513	0.510	0.507	0.524	0.040	0.042	0.040	0.041	0.038	0.041	0.038	0.038
0.457	0.447	0.447	0.446	0.039	0.039	0.040	0.040	0.038	0.038	0.038	0.038
0.552	0.532	0.536	0.530	0.042	0.043	0.043	0.043	0.038	0.039	0.039	0.040
0.463	0.456	0.446	0.448	0.041	0.041	0.041	0.042	0.038	0.038	0.039	0.038
0.452	0.432	0.435	0.427	0.073	0.073	0.073	0.074	0.047	0.047	0.047	0.047
0.456	0.440	0.454	0.437	0.069	0.070	0.069	0.070	0.047	0.047	0.047	0.047

Fluorescein (1.0s) (Counts)
988

3544	3949	3846	3817	3860	3746	4111	3948	3837	4175	4124	4223
687823	665819	656961	775118	13200	13600	13453	13615	12921	12925	12787	13210
323748	313306	309022	308494	14625	14785	15016	15110	12759	13081	13402	13416
10388	10292	9935	9947	10348	10223	10374	10253	10212	10746	10568	10751
6620	6942	6468	6492	10311	10325	10525	10470	10177	10539	10406	10650
13585	12959	12924	12676	19027	18921	19254	19589	20737	20475	20799	20718
14272	13933	15148	13734	15838	15759	16046	16178	20555	20846	20934	21083

Day 7 Time 4

A600 (Shell lab) (A)
-0.000

0.028	0.028	0.029	0.028	0.028	0.029	0.029	0.029	0.028	0.029	0.029	0.029
0.536	0.533	0.530	0.611	0.040	0.040	0.040	0.041	0.037	0.038	0.039	0.038
0.507	0.490	0.504	0.498	0.040	0.041	0.041	0.041	0.037	0.038	0.038	0.038
0.531	0.513	0.513	0.515	0.042	0.043	0.042	0.043	0.038	0.038	0.039	0.039
0.467	0.447	0.445	0.442	0.042	0.041	0.042	0.042	0.040	0.038	0.039	0.039
0.448	0.433	0.436	0.431	0.072	0.072	0.073	0.073	0.046	0.047	0.047	0.047
0.487	0.468	0.474	0.474	0.070	0.071	0.070	0.071	0.047	0.048	0.048	0.048

Fluorescein (1.0s) (Counts)
952

3552	3740	3729	3744	3988	3924	4212	4128	3800	4089	4069	4000
680117	661191	647560	3491590	13032	14043	13600	13975	12755	13253	13760	13346
373439	353370	355419	381649	22100	23256	23297	23231	13059	13474	13144	13769
9497	9191	9180	9083	9927	10358	10082	10156	10146	10487	10563	10832
7135	7062	6858	6792	10102	10314	10225	10372	10442	10410	10545	10843
15347	15293	15275	15226	18476	18541	18581	18830	20022	20835	20984	21009
275594	266860	271617	268862	30856	32324	31582	31312	22850	23497	23265	23807

Day 7 Time 24

A600 (Shell lab) (A)
-0.000

0.028	0.029	0.029	0.029	0.029	0.029	0.029	0.029	0.031	0.029	0.029	0.029
0.496	0.489	0.499	0.502	0.039	0.039	0.040	0.040	0.038	0.040	0.039	0.039
0.578	0.583	0.578	0.582	0.075	0.077	0.075	0.082	0.048	0.049	0.049	0.050
0.558	0.548	0.542	0.539	0.042	0.043	0.042	0.043	0.039	0.040	0.040	0.041
0.512	0.503	0.507	0.510	0.081	0.081	0.080	0.082	0.050	0.051	0.051	0.051
0.590	0.671	0.584	0.582	0.073	0.077	0.072	0.074	0.048	0.049	0.051	0.049
0.665	0.646	0.652	0.655	0.109	0.110	0.107	0.110	0.066	0.068	0.069	0.069

Fluorescein (1.0s) (Counts)
978

3536	3951	3850	3624	3680	3504	3571	3680	4050	4036	3675	3859
729690	716310	717602	725942	16453	16466	16933	16863	13579	13926	14378	14815
1005007	1018747	983283	1064537	150722	160247	150703	155636	18245	18578	18760	19397
11759	12317	11326	10917	9999	9990	9906	10055	10969	11311	11417	11723
10642	10393	10312	10360	14755	15022	14982	15509	11215	11487	11431	11453
20276	30388	19602	19578	19319	19255	19101	19278	21919	22428	22721	23437
3892809	3789378	3791768	3785920	462455	471240	457705	468707	60365	61843	63213	64995

Day 7 Time 72

0.028	0.029	0.029	0.029	0.028	0.029	0.029	0.030	0.029	0.029	0.029	0.029
0.529	0.524	0.530	0.524	0.039	0.039	0.039	0.039	0.038	0.038	0.038	0.038
0.540	0.508	0.526	0.563	0.079	0.104	0.089	0.090	0.050	0.051	0.052	0.052
0.529	0.519	0.522	0.525	0.042	0.042	0.042	0.042	0.038	0.039	0.039	0.039
0.530	0.503	0.570	0.526	0.090	0.083	0.082	0.083	0.053	0.054	0.059	0.054
0.532	0.515	0.518	0.518	0.070	0.071	0.071	0.072	0.046	0.047	0.047	0.047
0.594	0.572	0.576	0.580	0.108	0.108	0.106	0.108	0.082	0.083	0.085	0.085

Fluorescein (1.0s) (Counts)
973

3656	4153	3817	3777	4007	3664	4145	4804	3977	4285	3993	4251
804733	790553	790813	774946	21321	21052	21164	21946	14081	14531	14681	14826
838309	785200	796120	970148	122852	183269	141750	154662	11615	11944	11765	12578
15258	15243	14691	15099	9932	10192	10266	10145	11939	12445	12628	12887
13108	12558	14183	13863	27773	28057	28716	28210	12302	12595	13048	13081
16186	16033	15832	16027	19456	19903	20263	20344	23753	24490	24612	25144
3217615	3081165	3063464	3094794	553743	560422	555083	564138	28423	29264	29739	30494